

Published in final edited form as:

Cell Rep. 2012 July 26; 2(1): 52–61. doi:10.1016/j.celrep.2012.06.002.

Inhibitory Effects of Robo2 on Nephrin: A Crosstalk between Positive and Negative Signals Regulating Podocyte Structure

Xueping Fan^{1,5}, Qinggang Li^{1,5}, Anna Pisarek-Horowitz^{1,5}, Hila Milo Rasouly¹, Xiangling Wang¹, Ramon G. Bonegio¹, Hang Wang¹, Margaret McLaughlin², Steve Mangos², Raghu Kalluri³, Lawrence B. Holzman⁴, Iain A. Drummond², Dennis Brown², David J. Salant¹, and Weining Lu^{1,*}

¹ Renal Section, Department of Medicine, Boston University Medical Center, Boston, MA 02118, USA.

² Center for Systems Biology, Program in Membrane Biology and Division of Nephrology, Massachusetts General Hospital, Boston, MA 02114, USA.

³ Division of Matrix Biology, Beth Israel Deaconess Medical Center, Boston, MA 02115, USA.

⁴ Renal Electrolyte and Hypertension Division, University of Pennsylvania School of Medicine, Philadelphia, PA 19104, USA.

SUMMARY

Robo2 is the cell surface receptor for the repulsive guidance cue Slit and is involved in axon guidance and neuronal migration. Nephrin is a podocyte slit-diaphragm protein that functions in the kidney glomerular filtration barrier. Here we report that Robo2 is expressed at the basal surface of mouse podocytes and co-localizes with nephrin. Biochemical studies indicate that Robo2 forms a complex with nephrin in the kidney through adaptor protein Nck. In contrast to the role of nephrin that promotes actin polymerization, Slit2-Robo2 signaling inhibits nephrin-induced actin polymerization. In addition, the amount of F-actin associated with nephrin is increased in *Robo2* knockout mice that develop an altered podocyte foot process structure. Genetic interaction study further reveals that loss of Robo2 alleviates the abnormal podocyte structural phenotype in nephrin null mice. These results suggest that Robo2 signaling acts as a negative regulator on nephrin to influence podocyte foot process architecture.

INTRODUCTION

In the normal kidney, the trilaminar glomerular capillary wall, composed of fenestrated endothelial cells, basement membrane and podocytes, restricts the permeability to plasma proteins. Podocytes are specialized epithelial cells that extend primary and secondary processes to cover the outer surface of the glomerular basement membrane. The actin-rich interdigitating secondary processes, or foot processes, from neighboring podocytes create filtration slits bridged by a semi-porous slit-diaphragm that forms the final barrier to protein permeation. Whereas genetic mutations of podocyte slit-diaphragm proteins such as nephrin

© 2012 Elsevier Inc. All rights reserved.

*Correspondence should be addressed to: Assistant Professor of Medicine Renal Section, EBRC 538 Boston University Medical Center 650 Albany Street Boston, MA 02118, USA Tel: 617-414-1770 Fax: 617-638-7326 wlu@bu.edu.

⁵These authors contributed equally to this work.

Publisher's Disclaimer: This is a PDF file of an unedited manuscript that has been accepted for publication. As a service to our customers we are providing this early version of the manuscript. The manuscript will undergo copyediting, typesetting, and review of the resulting proof before it is published in its final citable form. Please note that during the production process errors may be discovered which could affect the content, and all legal disclaimers that apply to the journal pertain.

and others are associated with hereditary forms of proteinuric kidney disease (Tryggvason et al., 2006), it has become evident that the proteins that make up and associate with the slit-diaphragm are more than a simple structural barrier. These proteins form a balanced signaling network that may influence podocyte foot process structure and function through interaction with the F-actin cytoskeleton (Faul et al., 2007; Jones et al., 2006; Verma et al., 2006).

Roundabout (Robo) family proteins are cell surface receptors for the secreted ligand Slits (Dickson and Gilestro, 2006), which were originally found as repulsive guidance cues for axon pathfinding and migrating neurons during nervous system development (Guan and Rao, 2003). The transmembrane protein Robo2 contains five Ig motifs and three fibronectin type III (FNIII) repeats in its extracellular domain (Dickson and Gilestro, 2006). While both immunoglobulin (Ig) motifs 1 and 2 interact with Slit2, the first Ig1 motif of Robo2 is the primary binding site for Slit2 (Dickson and Gilestro, 2006). The intracellular domain of Robo2 has four cytoplasmic conserved (CC) sequences named CC0 to CC3 (Dickson and Gilestro, 2006). CC0 and CC1 contain conserved tyrosine residues, while CC2 and CC3 are proline-rich stretches. The repulsive Slit2-Robo2 signaling inhibits actin polymerization (Guan and Rao, 2003) or induces F-actin depolymerization (Piper et al., 2006).

Slit2-Robo2 signaling also plays crucial roles during early kidney induction and ureteric bud outgrowth. Mouse mutants that lack *Slit2* or *Robo2* develop supernumerary ureteric buds, which leads to a broad-spectrum of urinary tract anomalies (Grieshammer et al., 2004; Lu et al., 2007). Disruption of *ROBO2* in humans causes congenital anomalies of the kidneys and urinary tracts (CAKUT), and point mutations of *ROBO2* have been identified in patients with vesicoureteral reflux (VUR) (Lu et al., 2007). We recently showed that *Robo2* is crucial for the formation of a normal ureteral orifice and for the maintenance of an effective anti-reflux mechanism (Wang et al., 2011). However, it is not known if Robo2 also plays a role in the kidney after ureteric bud outgrowth.

Here, we report that Robo2 is a novel podocyte protein expressed at the basal surface of kidney podocytes and co-localizes with nephrin and podocin. Robo2 interacts directly with adaptor protein Nck SH3 domains and forms a complex with nephrin. In addition, Robo2 signaling inhibits actin polymerization induced by nephrin. Whereas Robo2 knockout mice develop altered podocyte foot processes, the loss of Robo2 alleviates the foot process structural abnormalities that are seen in nephrin null mice. These results suggest that Robo2 signaling acts as a negative regulator on nephrin signaling to influence podocyte foot process architecture.

RESULTS

Robo2 is a Novel Podocyte Protein Localized to the Basal Cell Surface of Mouse Podocytes

During kidney development, *Robo2* mRNA is expressed in the metanephric mesenchyme surrounding the ureteric bud and later in the proximal end of the S-shaped body (Piper et al., 2000), the location of primordial podocytes. This raises the possibility that Robo2 may also be involved in podocyte biology in addition to its role in early kidney induction. To investigate this, we performed in situ hybridization and found *Robo2* mRNA was expressed in the capillary loop stage of developing glomeruli of mouse embryos at embryonic day 16.5 (E16.5) (Figure S1A and S1B). Robo2 protein became detectable by immunofluorescence staining in the developing glomerulus around E14.5 and reached peak expression at E16.5 (Figure S1C–S1E). Although the expression decreased after E17.5 (Figure S1F), Robo2 expression was maintained in glomeruli after birth and was detectable in adult mice at 5 weeks of age (Figure S1G–S1H and S1L–S1M).

To determine the cellular localization of Robo2 in the developing glomerulus, we performed dual-label immunohistochemistry with glomerular cell type specific markers. We found that Robo2 protein was co-localized with nephrin (Figure 1A–1C) and podocin (Figure 1D–1F), two podocyte slit-diaphragm associated proteins. Robo2 was also co-expressed in the glomeruli with the nephrin-interacting adaptor protein Nck (Figure 1G–1I) and with WT1, a constituent of podocyte nuclei (Figure S1H–S1K). Dual-labeling with antibodies against nidogen, a basement membrane marker (Figure 1J–1L and 1P) and Pecam1, an endothelial cell marker (Figure 1M–1O; Figure S1M) showed that Robo2 was localized adjacent to the external surface of the glomerular basement membrane and absent from endothelial cells. High-resolution confocal microscopy further demonstrated that subcellular Robo2 was most abundant on the basal surface of podocytes (Figure 1Q). Immunogold electron microscopy of postnatal mouse kidneys with an antibody against the cytoplasmic domain established that Robo2 was localized to podocyte foot processes near to the cytoplasmic face of the slit-diaphragms (Figure 1R). These results demonstrate that Robo2 is a podocyte protein and its basal subcellular localization in the foot processes suggests that it may play a role in regulating podocyte foot process structure.

Robo2 Intracellular Domain Interacts Directly with SH3 Domains of the Adaptor Protein Nck

Nephrin extracellular domain engagement leads to tyrosine phosphorylation of its intracellular domain by Src kinases and recruitment of the SH2 domain of the adaptor protein Nck, which in turn induces actin polymerization (Jones et al., 2006; Verma et al., 2006). Nck harbors one SH2 domain in the C-terminus and three SH3 domains near the N-terminus. Actin polymerization is mediated by the SH3 domains of Nck (Rivera et al., 2004), which may recruit various cytoskeleton regulators including N-WASP and Pak (Jones et al., 2006). Interestingly, previous studies have shown that the SH3 domains of the *Drosophila* Nck homolog Dreadlock (Dock) also directly interact with the intracellular domain of Robo to inhibit actin polymerization (Fan et al., 2003). This prompted us to question whether mammalian Nck can also interact directly with Robo2 in the podocyte to regulate the F-actin cytoskeleton.

To address this possibility, we used a yeast two-hybrid assay to examine if Robo2 interacted with Nck. Since two mammalian Ncks (*i.e.* Nck1, Nck2) share similar structure and function in kidney development (Jones et al., 2006), we used Nck1 in this study and observed that the intracellular domain of Robo2 directly interacted with Nck1 (Figure 2A–2C). Binding site mapping in Robo2 for Nck1 showed that the sequence from amino acid 1085 to 1301, which contain 4 proline-rich motifs, was crucial for the interaction (Figure 2A and 2C). Absence of this proline-rich region prevented its interaction with Nck1 (Figure 2A). Binding site mapping in Nck1 for Robo2 showed that the first two SH3 domains were required for its interaction with Robo2 because deleting either or both of them abrogated the interaction (Figure 2B). Thus, Robo2 and Nck1 interaction was mediated by two well-characterized protein domains: the SH3 domains and proline-rich motifs (Figure 2C). CD2AP, another podocyte adaptor protein, also bears three SH3 domains in its N-terminus (Shih et al., 2001), but we did not detect any interaction between CD2AP and Robo2 in either the yeast two-hybrid or co-precipitation assays (data not shown). These observations suggest that the binding between Robo2 and Nck1 in the podocyte is a specific interaction.

Full-Length Robo2 Forms a Complex with Nephrin through Nck

We confirmed the interaction between Robo2 and Nck by pull down and co-precipitation assays. His- and myc-tagged human full-length Robo2 (His-myc-Robo2) or his- and myc-tagged human Robo2 with a deletion of the Nck1 binding domain (His-myc-Robo2- Δ NBD) were expressed in HEK (293T) cells. Transfected HEK cells were stimulated with Slit2

conditioned medium (prepared from Slit2 stably transfected cells) to activate Robo2 and increase Nck binding (Fan et al., 2003). Nck was pulled down with His-myc-Robo2 from the HEK cell lysates using Ni-NTA beads but not with His-myc-Robo2-NBD (Figure 2D). Since the SH2 domain of Nck interacts with phosphotyrosines in the nephrin cytoplasmic domain (NCD) (Jones et al., 2006; Verma et al., 2006), we examined whether Robo2 formed a complex with nephrin through Nck using a co-precipitation assay. To establish proof of principle, we co-expressed Robo2 and nephrin in HEK cells with Fyn kinase to increase nephrin phosphorylation (Verma et al., 2006). Pull-down of His-myc-Robo2 (but not of His-myc-Robo2- Δ NBD) from the HEK cell lysates with Ni-NTA beads co-precipitated Nck and nephrin when Fyn was expressed (Figure 2E). In the reverse order, pulling down His-myc-nephrin co-precipitated Nck and Robo2 when Fyn kinase was expressed (Figure 2F). Furthermore, the precipitates prepared with the anti-Nck antibody contained both Robo2 and nephrin when Fyn was over-expressed (Figure S2A). These data suggest that nephrin, Nck, and Robo2 form a complex in vitro. To validate these findings in vivo, we immunoprecipitated Robo2 from newborn mouse kidney lysates and found that Nck and nephrin were co-precipitated (Figure 2G). Conversely, the precipitates prepared with the anti-nephrin antibody also contained Nck and Robo2 (Figure 2H). Since nephrin is uniquely expressed in podocytes of kidney lysates, and Nck and Robo2 are also localized in these cells in the kidney, these results indicate that nephrin, Nck, and Robo2 are able to form a complex in podocytes.

To determine the role of Slit2 in the formation of the Robo2-Nck-nephrin protein complex, His-myc-Robo2, nephrin, and Fyn were co-expressed in HEK cells that were stimulated with Slit2 conditioned medium or control conditioned medium without Slit2 prior to co-precipitation (Figure 2I). We observed that Slit2 stimulation increased Robo2 binding to Nck and complex formation with nephrin. Both ratios of Nck1 versus Robo2 and nephrin versus Robo2 were increased after Slit2 stimulation (Figure 2J). Consistent with this finding, we observed that Slit2 was also expressed in newborn and adult mouse glomeruli (Figure S2B and S2C).

Slit2-Robo2 Signaling Inhibits Nephrin-Induced Actin Polymerization

Since Slit binds Robo to recruit Dock and srGAPs, thereby inhibiting actin polymerization (Fan et al., 2003; Wong et al., 2001), we wondered if Robo2 might also recruit Nck to inhibit actin polymerization in mammalian cells, an opposite role to nephrin that promotes actin polymerization. To address this question, we studied actin polymerization by analyzing F-actin tails in cells expressing the CD16/7-NCD chimeric protein as previously described (Jones et al., 2006; Verma et al., 2006). This model utilizes the extracellular and transmembrane domains of the human immunoglobulin Fc receptors CD16 and CD7 fused to the nephrin cytoplasmic domain (NCD). CD16/7-HA, in which NCD was replaced by an HA tag, was used as a negative control. These chimeric proteins were co-expressed with Robo2 in HEK cells and clustered by treatment with anti-CD16 antibody and a secondary antibody conjugated to rhodamine. We first examined if clustering of the nephrin cytoplasmic domain could recruit Robo2 in the presence of Slit2. We observed that engagement of CD16/7-NCD moved nephrin into the Robo2 complexes since most of the Robo2 colocalized with the CD16/7-NCD clusters (Figure S2D, S2E, S2F). However, no colocalization of the Robo2 was observed either with the CD16/7-HA control (Figure S2D') or with the Robo2- Δ NBD construct (Figure S2E'), in which the Robo2 Nck binding domain (NBD) was deleted. Interestingly, in the absence of Slit2, colocalization of CD16/7-NCD and Robo2 was significantly reduced (Figure S2F'). These data provide further evidence that the nephrin cytoplasmic domain is able to complex with the Robo2 intracellular domain in the presence of Slit2 and validates the model to determine if the formation of a Robo2-Nck-nephrin complex affects actin polymerization.

HEK cells expressing CD16/7-NCD and Robo2 were stimulated with Slit2 or control conditioned medium while clustered by the anti-CD16 antibody. Actin polymerization was evaluated by quantifying the number of HEK cells with visible F-actin tails (Rivera et al., 2004). We observed that ~80% of the CD16/7-NCD clustered cells formed F-actin tails that could be revealed by phalloidin staining as previously reported (Jones et al., 2006; Verma et al., 2006). Upon Slit2 stimulation, however, the number of cells with F-actin tails was significantly reduced to approximately 40% (Figure 3A and 3C). Only a few cells were observed to contain F-actin tails when the control CD16/7-HA proteins were clustered (Figure 3B and 3C). To further investigate whether this inhibition of actin polymerization required Nck, we repeated this assay using Robo2 without Nck binding domain (Robo2- Δ NBD) to determine if blocking of Nck binding to Robo2 would prevent Slit2-Robo2 inhibition on nephrin-induced actin polymerization. CD16/7-NCD was co-expressed with either full-length Robo2 (Figure S3A) or Robo2- Δ NBD (Figure S3B) in HEK cells. We observed that deletion of the Nck binding domain in Robo2 significantly compromised Slit2-Robo2 inhibition on nephrin-induced actin polymerization (Figure S3C).

A previous study shows that nephrin is linked to the F-actin cytoskeleton (Yuan et al., 2002). To determine if Slit2-Robo2 signaling could inhibit the association of F-actin and nephrin, we immunoprecipitated CD16/7-NCD and CD16/7-HA with anti-CD16 antibody and examined the amount of F-actin in the precipitates by Western blot. We observed that the abundance of F-actin associated with nephrin was significantly reduced upon Slit2 stimulation (Figure 3D and 3E). Conversely, in vivo immunoprecipitation assay showed that F-actin associated with nephrin immunoprecipitated by an anti-nephrin antibody from *Robo2* newborn null mouse kidneys was significantly increased compared with that from wild type or *Robo2* heterozygous mouse kidneys (Figure 3F and 3G). Taken together, these results indicate that Slit2-Robo2 signaling inhibits nephrin-induced actin polymerization.

Loss of Robo2 in Podocytes Causes Altered Foot Process Structure in Mice

We and others have previously shown that almost all *Robo2* homozygous null mice in mixed genetic background die shortly after birth due to a severe CAKUT phenotype (Grieshammer et al., 2004; Lu et al., 2007; Wang et al., 2011). After breeding mice with a *Robo2* ^{Δ del5} (also called *Robo2*⁻) mutant allele for five generations onto C57BL/6 genetic background, mating of *Robo2*^{del5/+} heterozygous parents revealed three *Robo2*^{del5/del5} homozygous mice that survived to 3 weeks (among a total of 160 mice analyzed at weaning). To determine if *Robo2* is required for podocyte foot process formation during development, we examined the ultrastructure of glomeruli in *Robo2* null mice at birth and 3 weeks of age. Although the podocyte body, foot processes and slit-diaphragm were formed at birth, transmission electron microscopy showed focal foot process effacement in newborn *Robo2*^{del5/del5} homozygous mice (Figure S4A-S4F). By scanning electron microscopy, we observed irregular interdigitating foot processes in *Robo2*^{del5/del5} homozygous null mice at birth and 3 weeks of age (Figure 4A-4H). These findings suggest that Robo2 plays a role in normal podocyte foot process patterning during kidney development.

To examine the role of Robo2 in the maintenance of foot process structure in mature glomeruli, we generated podocyte specific *Robo2* knockout mice by crossing conditional *Robo2*^{flox/flox} mice with *Robo2*^{del5/+}; *Tg*^{Nphs2-Cre/+} heterozygous mice carrying a podocin-Cre transgene. Twenty podocyte specific *Robo2* mutant mice with *Robo2*^{del5/flox}; *Tg*^{Nphs2-Cre/+} genotype and 20 littermate control mice were analyzed up to one year of age. Podocyte specific *Robo2* knockout mice were viable and fertile. However, they displayed unusually broad podocyte foot processes and focal segmental foot process effacement at one month (Figure 4I-4M). At 6 weeks of age the mutant mice developed microalbuminuria, which was detected by both ELISA and Western blot analyses (Figure 4N and 4O). In addition, scanning electron microscopy revealed foot process patterning

changes in *Robo2* podocyte specific knockout mice. Instead of orderly zipper-like interdigitating secondary foot processes in the wild-type, *Robo2* podocyte specific knockout mice displayed irregular and disorganized foot process interdigitation patterns at one month (Figure S4G-S4J). These changes became more obvious over time. At seven months of age, overtly disorganized, shorter, and meandering foot processes were observed (Figure S4K-S4N), which were similar to the phenotype of three-week old *Robo2* null mice. Although *Robo2* podocyte specific knockout mice had normal podocyte number, matrix deposition was significantly increased in glomeruli (Figure S4O-S4T, Table S1 and S2). These morphological and functional changes suggest that *Robo2* plays a role in regulating and maintaining glomerular podocyte foot process structure.

Loss of *Robo2* Alleviates the Podocyte Structural Defect in Nephrin Null Mice

Nephrin is capable of inducing localized actin polymerization under physiological conditions (Jones et al., 2006; Verma et al., 2006). Nephrin homozygous mice develop a characteristic phenotype with dilation of the Bowman's space, abnormally broad foot processes, absence of glomerular slit-diaphragms, and significant proteinuria (Done et al., 2008; Hamano et al., 2002). Since *Robo2* formed a complex with nephrin, and *Slit2*-*Robo2* signaling inhibited nephrin-induced actin polymerization, we wondered if loss of *Robo2* would modify the podocyte phenotype in nephrin null mice. To test this hypothesis of a possible genetic interaction between *Robo2* and nephrin, we generated both germline *Robo2*^{-/-}; *Nphs1*^{-/-} and podocyte-specific *Robo2*^{lox/flox}; *Tg*^{Nphs2-Cre/+}; *Nphs1*^{-/-} double *Robo2*-nephrin knockout mice. Like *Nphs1*^{-/-} single homozygote, both *Robo2*^{-/-}; *Nphs1*^{-/-} (4/4, 100%) and *Robo2*^{lox/flox}; *Tg*^{Nphs2-Cre/+}; *Nphs1*^{-/-} (3/3, 100%) double knockout mice died within 10 hours after birth. Histological analysis, however, revealed that the morphology of glomeruli in the *Robo2*^{-/-}; *Nphs1*^{-/-} double homozygous mice appeared relatively normal compared with the phenotype in *Nphs1*^{-/-} single nephrin homozygous mice, which had a dilated Bowman's space (Figure S4U-S4X). The number of glomeruli with dilated Bowman's space was significantly reduced in *Robo2*^{-/-}; *Nphs1*^{-/-} double homozygous mice (2/55, 3.6%) compared with nephrin single null mice (31/122, 25.4%) (Figure S4Y, and Table S3). In addition, analysis of glomerular ultrastructure by scanning electron microscopy showed that the interdigitating podocyte foot process structure was observed in only 1 (6.67%) of 15 glomeruli from nephrin single homozygous mice (Figure 4P and 4Q) compared with 100% in *Robo2*^{-/-} single homozygotes (Figure 4T and 4U) and wild-type controls (Figure 4V and 4W). Remarkably, the interdigitating pattern of the podocyte foot processes was restored in 12 (75%) of 16 glomeruli from *Robo2*^{-/-}; *Nphs1*^{-/-} double homozygous newborn mouse kidneys (Figure 4R and 4S, Table S4), suggesting that a concomitant loss of *Robo2* and nephrin alleviated the podocyte foot process structural phenotype in these mice. These findings indicate that the *Robo2*-Nck-nephrin physical interactions described above have a substantial effect on podocyte foot process morphology in vivo when the levels of expression of *Robo2* and nephrin are genetically altered.

DISCUSSION

Podocytes exhibit a remarkable degree of plasticity. During development they differentiate from simple cuboidal epithelial cells into the elaborate process-bearing cells that we recognize as mature podocytes (Reeves et al., 1978). This plasticity is retained after maturation. It is seen most graphically as reversible foot process effacement following experimental surface charge neutralization with protamine sulfate and restoration with heparin (Seiler et al., 1975) and during relapse and remission of proteinuria in children with minimal change disease (Nachman et al., 2008). More subtle changes in foot processes probably occur under physiological conditions in response to positive and negative signals in the form of hemodynamic, hormonal or paracrine stimuli. Given the abundance of F-actin

in the foot processes, it is likely that such stimuli bring about those subtle changes in response to positive and negative signals transduced to the F-actin cytoskeleton. Too much or unbalanced positive signals may lead to disease phenotype. Indeed, although a physiological ligand has yet to be identified, it is now clear that clustering and phosphorylation of nephrin induces actin polymerization by recruiting Nck. This mechanism may be involved in the proteinuria induced in rats by a nephritogenic monoclonal antibody to the extracellular domain of nephrin (Topham et al., 1999) and in cases of congenital nephrotic syndrome that develop anti-nephrin alloantibodies after renal transplantation (Pattrakka et al., 2002).

Our studies reveal another level of negative regulation of podocyte actin polymerization in which Robo2, when bound by Slit, inhibits nephrin-induced actin polymerization. While the precise mechanisms have yet to be defined, we propose that Slit-Robo2 signaling might inhibit nephrin-induced actin polymerization to maintain normal podocyte foot process structure as follows: Under physiological conditions (e.g. during foot process development), nephrin engagement leads to phosphorylation of the intracellular Y1191/1208/1232 to which the Nck SH2 domain binds (Jones et al., 2006; Verma et al., 2006). Nck in turn recruits cytoskeleton regulators such as N-WASP through its SH3 domains to promote actin polymerization for podocyte foot-process extension or spreading (Figure S4Z). Local secretion and binding of Slit increases the interaction of Robo2 with Nck through its proline rich region and the first two SH3 domains of Nck. Sequestering the first two SH3 domains of Nck by Robo2 would inhibit actin polymerization and decrease F-actin associated with nephrin to maintain a dynamic and balanced F-actin cytoskeleton and normal podocyte foot process structure (Figure S4Z). In addition to direct inhibition of nephrin-induced actin polymerization through Nck, Slit-Robo2 signaling may inactivate actin polymerization through other pathways such as recruiting Ena, Abl, srGAPs to negatively regulate F-actin cytoskeleton (Bashaw et al., 2000; Wong et al., 2001). In the absence of Slit-Robo2 signaling (e.g. when Robo2 is knocked out), the inhibitory effect of Robo2 on nephrin induced polymerization is lost. The SH3 domains of Nck are able to interact with downstream cytoskeletal regulators to increase actin polymerization (Figure S4Z), which may explain the altered podocyte foot process structure identified in *Robo2* mutant mice. Our results thus support the concept that Slit-Robo signaling may regulate podocyte plasticity by negatively regulating F-actin cytoskeleton, which is similar to the role of Slit-Robo signaling in axon growth cone pathfinding (Guan and Rao, 2003). The pathological finding of increased matrix deposition in the *Robo2* mutant mouse glomeruli likely represents a secondary response although the mechanisms and consequences have yet to be defined.

Although it is clear from our studies that Robo2 localizes to the basal surface of podocytes and forms a complex with other established foot process slit-diaphragm proteins through its intracellular domain, it remains uncertain if it actually forms part of the slit-diaphragm itself. Interestingly, the extracellular domain of Robo2 resembles that of nephrin, which has eight immunoglobulin (Ig)-like motifs and one fibronectin domain whereas Robo2 has five Ig-like motifs and three fibronectin domains (Figure S4Z) (Tryggvason et al., 2006). We have tested the interaction between the intracellular domain of Robo2 and the cytoplasmic domain of nephrin in the yeast two-hybrid assay but did not observe any positive results. Our biochemical data (Figure 2E and 2F) also did not support a direct interaction between these two receptors in vitro. However, we cannot exclude the possibility that the extracellular domain of Robo2 may associate with the extracellular domain of nephrin in vivo on the cell membranes of adjacent foot processes through a trans-interaction in the slit-diaphragm.

We found that *Robo2* knockout mice developed an altered foot process interdigitating pattern, a phenotype that is different from that of the nephrin null mice (Done et al., 2008; Hamano et al., 2002). This is not surprising since nephrin and *Robo2* play opposite roles in regulating the podocyte F-actin cytoskeleton. While nephrin signaling induces localized actin polymerization, Slit2-*Robo2* signaling acts as a negative regulator on nephrin induced actin polymerization to maintain podocyte foot process plasticity and dynamics. It is noteworthy that a similar foot process organization defect is observed in mice in which the actin-depolymerizing factor Cofilin-1, another negative regulator of the F-actin cytoskeleton in podocytes, is knocked out (Garg et al., 2010). This suggests that the absence of either an actin polymerization promoting factor such as nephrin or an inhibitory factor such as *Robo2* will affect the normal structure of podocytes. Thus the balance between positive and negative F-actin cytoskeleton regulators in podocytes is important to maintain normal foot process structure. Regaining this balance by knocking out both positive and negative signals may explain the restoration of podocyte foot process interdigitation in the *Robo2*-nephrin double knockout mice. Our studies highlight the dual roles of nephrin as an essential component of the slit-diaphragm to control glomerular permselectivity on the one hand (Tryggvason et al., 2006) and as a regulator of foot process morphology through its interaction with the actin cytoskeleton (Jones et al., 2006; Verma et al., 2006) on the other. While *Robo2* signaling clearly counters the positive signaling effects of nephrin on the foot processes, it remains to be determined if it also influences slit-diaphragm integrity.

In summary, we have identified *Robo2* as a new component of the podocyte intercellular junction in the kidney. We have demonstrated interactions between *Robo2* and nephrin using biochemical, functional, and genetic techniques, and have shown that Slit2-*Robo2* signaling inhibits nephrin-induced actin dynamics. Our results suggest that *Robo2* signaling acts as a negative regulator on nephrin signaling to modulate podocyte foot process architecture. This study extends our understanding of the role of Slit-*Robo* signaling and identifies a novel crosstalk mechanism by which guidance cue receptor *Robo* might influence F-actin cytoskeleton dynamics. Further studies are needed to determine if eliminating or blocking Slit2-*Robo2* signaling can be used therapeutically to restore podocyte foot process structure in those diseases in which nephrin expression is reduced (Furness et al., 1999).

OVERVIEW EXPERIMENTAL PROCEDURES

Detailed information can be found in the Extended Experimental Procedures in Supplemental Information.

Tissue in Situ Hybridization, Immunohistochemistry, and Immunogold Electron Microscopy

In situ hybridization analysis was performed with digoxigenin-labeled *Robo2* riboprobes as previously described (Grieshammer et al., 2004). Immunohistochemistry was performed on mouse embryonic kidney tissues fixed in 4% paraformaldehyde and in adult mouse kidney tissues fixed in methanol. For immunogold electron microscopy, wild-type mouse kidneys were dissected and fixed in paraformaldehyde-lysine-periodate (PLP). Ultrathin sections of the mouse kidney were prepared and incubated with goat anti-*Robo2* antibody (DAKO Corporation) and a secondary antibody coupled to 10 nm colloidal gold (Ted Pella).

Yeast Two-Hybrid, Co-Precipitation, and Actin Polymerization Assays

The DupLEX-A™ yeast two-hybrid system (OriGene Tech) was used to characterize *Robo2* and Nck1 interaction according to manufacturer's instructions. Cell culture, His-tagged protein co-precipitation, and immunoprecipitation were performed as previously reported

(Fan et al., 2003). For endogenous immunoprecipitation, mouse newborn kidneys were utilized. CD16 antibody-mediated crosslinking of CD16/7 fusion proteins and the actin polymerization assay were performed as previously described (Jones et al., 2006; Rivera et al., 2004; Verma et al., 2006).

Knockout Mouse study, Transmission and Scanning Electron Microscopy, and Kidney Glomerular Analysis

The generation and genotyping of *Robo2*^{fllox} conditional allele, *Robo2*^{del5} (also called *Robo2*⁻ interchangeably in this paper) germline mutant allele, and *Robo2*⁺ wild-type allele were described previously (Lu et al., 2007; Wang et al., 2011). To generate *Robo2*-nephrin double knockout mice, *Robo2*^{+/-} mice were crossed with *Nphs1*^{+/-} mice that were generated previously (Hamano et al., 2002). For transmission electron microscopy, kidneys were fixed, incubated in 2% glutaraldehyde in 0.15 M sodium cacodylate, dehydrated in graded ethanol, embedded in Epon, sectioned, and stained with uranyl acetate and lead citrate. Ultrathin kidney sections were examined using a JEM-1011 electron microscope. For scanning electron microscopy, kidneys were prepared following the standard protocol. For kidney pathological studies, kidneys were fixed in 4% paraformaldehyde, paraffin embedded, sectioned, and stained using standard Periodic acid-Schiff (PAS) or eosin hematoxylin (H&E) methods. For quantification of podocyte number, WT1 was used as a podocyte nuclear marker and immunoperoxidase staining was performed on kidney sections following the standard protocol. WT1 positive podocyte nuclei in each glomerular cross section were counted. For proteinuria analysis, “spot” urine specimens from 6 weeks old mice were examined using a murine albuminuria ELISA quantitation kit (Exocell) according to manufacturer’s instruction and urine dipstick (Multistix, Bayer, IN) as a screening method.

Supplementary Material

Refer to Web version on PubMed Central for supplementary material.

Acknowledgments

We thank Ms Juan Liu for technical assistance; Dr. Uta Grieshammer for providing *Robo2* riboprobe plasmid; Drs. Herbert Cohen and William Andrews for providing *Nphs1* and *Robo2* cDNA; Drs. Dezhi Wang and Zhifeng Ren for help with EM facility; and Dr. Peleg Horowitz for critical reading of this manuscript. This work is supported by NIH grants R01DK078226 (to W.L.) and R01DK30932 (to D.J.S.), and is also supported in part by Research Grant #6-FY08-304 from the March of Dimes Foundation (to W.L.).

REFERENCES

- Bashaw GJ, Kidd T, Murray D, Pawson T, Goodman CS. Repulsive axon guidance: Abelson and Enabled play opposing roles downstream of the roundabout receptor. *Cell*. 2000; 101:703–715. [PubMed: 10892742]
- Dickson BJ, Gilestro GF. Regulation of commissural axon pathfinding by slit and its Robo receptors. *Annu Rev Cell Dev Biol*. 2006; 22:651–675. [PubMed: 17029581]
- Done SC, Takemoto M, He L, Sun Y, Hultenby K, Betsholtz C, Tryggvason K. Nephrin is involved in podocyte maturation but not survival during glomerular development. *Kidney Int*. 2008; 73:697–704. [PubMed: 18046313]
- Fan X, Labrador JP, Hing H, Bashaw GJ. Slit stimulation recruits Dock and Pak to the roundabout receptor and increases Rac activity to regulate axon repulsion at the CNS midline. *Neuron*. 2003; 40:113–127. [PubMed: 14527437]
- Faul C, Asanuma K, Yanagida-Asanuma E, Kim K, Mundel P. Actin up: regulation of podocyte structure and function by components of the actin cytoskeleton. *Trends Cell Biol*. 2007; 17:428–437. [PubMed: 17804239]

- Furness PN, Hall LL, Shaw JA, Pringle JH. Glomerular expression of nephrin is decreased in acquired human nephrotic syndrome. *Nephrol Dial Transplant*. 1999; 14:1234–1237. [PubMed: 10344367]
- Garg P, Verma R, Cook L, Soofi A, Venkatareddy M, George B, Mizuno K, Gurniak C, Witke W, Holzman LB. Actin-depolymerizing factor cofilin-1 is necessary in maintaining mature podocyte architecture. *J Biol Chem*. 2010; 285:22676–22688. [PubMed: 20472933]
- Grieshammer U, Le M, Plump AS, Wang F, Tessier-Lavigne M, Martin GR. SLIT2-mediated ROBO2 signaling restricts kidney induction to a single site. *Dev Cell*. 2004; 6:709–717. [PubMed: 15130495]
- Guan KL, Rao Y. Signalling mechanisms mediating neuronal responses to guidance cues. *Nat Rev Neurosci*. 2003; 4:941–956. [PubMed: 14682358]
- Hamano Y, Grunkemeyer JA, Sudhakar A, Zeisberg M, Cosgrove D, Morello R, Lee B, Sugimoto H, Kalluri R. Determinants of vascular permeability in the kidney glomerulus. *J Biol Chem*. 2002; 277:31154–31162. [PubMed: 12039968]
- Jones N, Blasutig IM, Eremina V, Ruston JM, Bladt F, Li H, Huang H, Larose L, Li SS, Takano T, et al. Nck adaptor proteins link nephrin to the actin cytoskeleton of kidney podocytes. *Nature*. 2006; 440:818–823. [PubMed: 16525419]
- Lu W, van Eerde AM, Fan X, Quintero-Rivera F, Kulkarni S, Ferguson HL, Kim H, Fan Y, Xi Q, Li QG, et al. Disruption of ROBO2 is associated with urinary tract anomalies and confers risk of vesicoureteral reflux. *Am J Hum Genet*. 2007; 80:616–632. [PubMed: 17357069]
- Nachman, PH.; Jennette, JC.; Falk, RJ. Primary glomerular disease. In: Brenner, BM., editor. *Brenner & Rector's The Kidney*. Saunders; Philadelphia: 2008. p. 987-1066.
- Patrakka J, Ruotsalainen V, Reponen P, Qvist E, Laine J, Holmberg C, Tryggvason K, Jalanko H. Recurrence of nephrotic syndrome in kidney grafts of patients with congenital nephrotic syndrome of the Finnish type: role of nephrin. *Transplantation*. 2002; 73:394–403. [PubMed: 11884936]
- Piper M, Anderson R, Dwivedy A, Weinl C, van Horck F, Leung KM, Cogill E, Holt C. Signaling mechanisms underlying Slit2-induced collapse of *Xenopus* retinal growth cones. *Neuron*. 2006; 49:215–228. [PubMed: 16423696]
- Piper M, Georgas K, Yamada T, Little M. Expression of the vertebrate Slit gene family and their putative receptors, the Robo genes, in the developing murine kidney. *Mech Dev*. 2000; 94:213–217. [PubMed: 10842075]
- Reeves W, Caulfield JP, Farquhar MG. Differentiation of epithelial foot processes and filtration slits: sequential appearance of occluding junctions, epithelial polyanion, and slit membranes in developing glomeruli. *Lab Invest*. 1978; 39:90–100. [PubMed: 682603]
- Rivera GM, Briceno CA, Takeshima F, Snapper SB, Mayer BJ. Inducible clustering of membrane-targeted SH3 domains of the adaptor protein Nck triggers localized actin polymerization. *Curr Biol*. 2004; 14:11–22. [PubMed: 14711409]
- Seiler MW, Venkatachalam MA, Cotran RS. Glomerular epithelium: structural alterations induced by polycations. *Science*. 1975; 189:390–393. [PubMed: 1145209]
- Shih NY, Li J, Cotran R, Mundel P, Miner JH, Shaw AS. CD2AP localizes to the slit diaphragm and binds to nephrin via a novel C-terminal domain. *Am J Pathol*. 2001; 159:2303–2308. [PubMed: 11733379]
- Topham PS, Kawachi H, Haydar SA, Chugh S, Addona TA, Charron KB, Holzman LB, Shia M, Shimizu F, Salant DJ. Nephritogenic mAb 5-1-6 is directed at the extracellular domain of rat nephrin. *J Clin Invest*. 1999; 104:1559–1566. [PubMed: 10587519]
- Tryggvason K, Patrakka J, Wartiovaara J. Hereditary proteinuria syndromes and mechanisms of proteinuria. *N Engl J Med*. 2006; 354:1387–1401. [PubMed: 16571882]
- Verma R, Kovari I, Soofi A, Nihalani D, Patrie K, Holzman LB. Nephrin ectodomain engagement results in Src kinase activation, nephrin phosphorylation, Nck recruitment, and actin polymerization. *J Clin Invest*. 2006; 116:1346–1359. [PubMed: 16543952]
- Wang H, Li Q, Liu J, Mendelsohn C, Salant DJ, Lu W. Noninvasive assessment of antenatal hydronephrosis in mice reveals a critical role for Robo2 in maintaining anti-reflux mechanism. *PLoS One*. 2011; 6:e24763. [PubMed: 21949750]

- Wong K, Ren XR, Huang YZ, Xie Y, Liu G, Saito H, Tang H, Wen L, Brady-Kalnay SM, Mei L, et al. Signal transduction in neuronal migration: roles of GTPase activating proteins and the small GTPase Cdc42 in the Slit-Robo pathway. *Cell*. 2001; 107:209–221. [PubMed: 11672528]
- Yuan H, Takeuchi E, Salant DJ. Podocyte slit-diaphragm protein nephrin is linked to the actin cytoskeleton. *Am J Physiol Renal Physiol*. 2002; 282:F585–591. [PubMed: 11880318]

HIGHLIGHTS

- Robo2 is a novel podocyte protein that co-localizes with nephrin
- Robo2 forms a complex with nephrin through Nck
- Slit2-Robo2 signaling inhibits nephrin-induced actin polymerization
- Loss of Robo2 alleviates podocyte structural phenotype in nephrin mutant mice

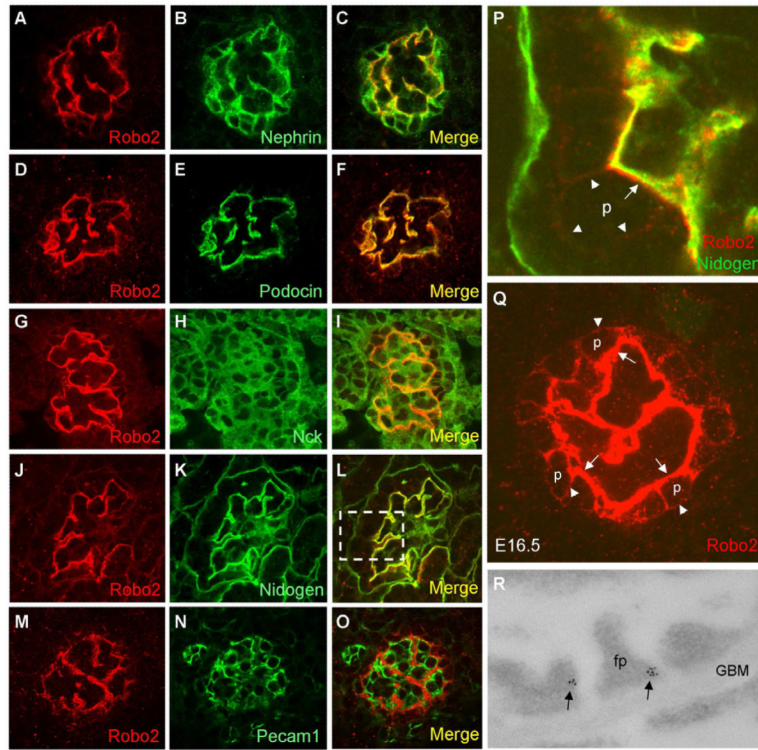


Figure 1. Robo2 is expressed and localized to the basal cell surface of podocytes

All immunostainings in (A-Q) are performed at mouse E16.5 days at 600X magnification (see Figure S1 for immunostainings in adult mouse glomeruli).

(A–C) Robo2 co-localizes with podocyte slit-diaphragm protein nephrin.

(D–F) Robo2 co-localizes with podocyte slit-diaphragm protein podocin.

(G–I) Robo2 co-localizes with adaptor protein Nck in glomeruli.

(J–L) Robo2 is expressed on the basal podocyte surface adjacent to glomerular basement membrane protein nidogen.

(M–O) Robo2 does not co-localize with glomerular endothelial cell protein marker Pecam1.

(P) The enlarged region boxed in (L) shows that Robo2 (red) is expressed predominantly on the basal cell surface (arrow) of podocytes (p) adjacent to glomerular basement membrane marker nidogen (green). Robo2 is weakly expressed in the apical and lateral cell surfaces (arrowheads) of podocytes.

(Q) Robo2 is expressed predominantly on the basal cell surface (arrows) of podocytes (p) and is weakly expressed on the apical or lateral cell surfaces (arrowheads).

(R) Immunogold electron microscopy shows localization of gold partials (arrows) conjugated to Robo2 antibody in the foot process (fp) of a podocyte from a 3-week old mouse. GBM, glomerular basement membrane. Magnification: 50,000X. See also Figure S1.

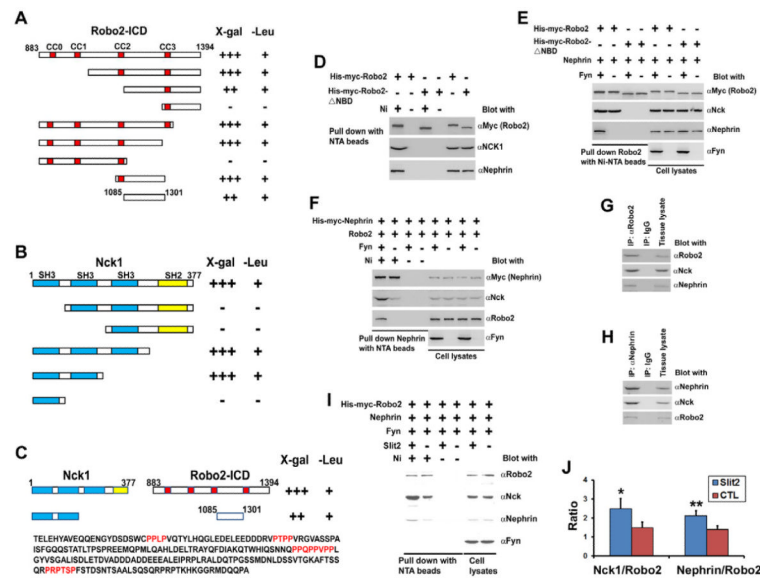


Figure 2. Robo2 interacts with the adapter protein Nck and forms a complex with nephrin

(A) Yeast two-hybrid assays show a positive interaction between Robo2 intracellular domain (Robo2-ICD) and Nck1. *LacZ* reporter (X-gal): +++, yeast turned dark blue; ++, light blue; -, white in 24 hours. Leucine reporter (-Leu): +, yeast grew; -, yeast did not grow. CC, cytoplasmic conserved region. Numbers indicate residue positions in the full-length protein.

(B) Yeast two-hybrid assays show the first two SH3 domains of Nck1 are required for its interaction with Robo2-ICD.

(C) Yeast two-hybrid assays show the potential binding domains that mediate Robo2 and Nck1 interaction. The sequence is the potential binding region in Robo2 for Nck1. Proline-rich regions are highlighted in red.

(D) Co-precipitation of Robo2 and Nck. Cell lysates in lane 5 are collected from His-myc-Robo2 transfected cells (used in lanes 1 and 2); Cell lysates in lane 6 are collected from His-myc-Robo2-ΔNBD transfected cells (used in lanes 3 and 4).

(E) Co-precipitation of Robo2, Nck, and nephrin. (F) A similar co-precipitation as (E) except that His-myc-nephrin is pulled-down instead of His-myc-Robo2.

(G) Co-immunoprecipitation of kidney endogenous Robo2, Nck, and nephrin.

(H) A similar assay as (G) except that precipitates are prepared using mouse anti-nephrin antibody.

(I) Slit2 enhances Robo2-Nck-nephrin complex formation. His-myc-Robo2, nephrin, and Fyn are expressed in HEK cells that are stimulated with Slit2 conditioned medium (lanes 1, 3) or control conditioned medium (lane 2, 4).

(J) Intensity quantification of (I). Data are represented as mean ± SEM; $n=7$, * $p < 0.05$, ** $p < 0.01$ compared with the control, paired student's *t*-test. See also Figure S2.

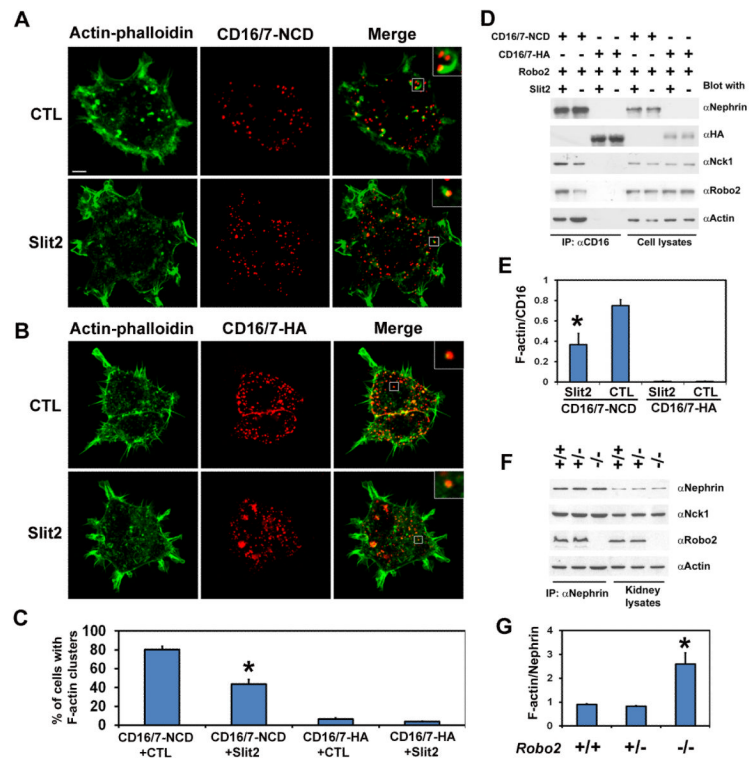


Figure 3. Slit2-Robo2 signaling inhibits nephrin-mediated actin polymerization

(A) CD16/7-NCD is co-expressed with Robo2 in HEK cells, which are treated with anti-CD16 antibody and rhodamine-conjugated anti-IgG antibody in the presence of Slit2 conditioned medium (Slit2) or control conditioned medium (CTL). Cells are then fixed and stained with FITC-conjugated phalloidin to reveal F-actin. Scale bar, 5 μ m. NCD: nephrin cytoplasmic domain.

(B) A similar assay as (A) except that CD16/7-NCD is replaced by CD16/7-HA and is used as a control assay.

(C) The percentage of cells with F-actin tails over total cells with CD16/7 clusters in each group is quantified. Data are represented as mean \pm SEM, * p < 0.01, n =5.

(D) CD16/7-NCD in (A) is immunoprecipitated by anti-CD16 antibody after Slit2 conditioned medium stimulation (lanes 1 and 3) or control conditioned medium (lanes 2 and 4). Note reduced F-actin in lane 1. CD16/7-HA is used as a negative control.

(E) Intensity quantification of (D). Data are represented as mean \pm SEM; n =4, * p < 0.05 compared with the control, paired student's t -test.

(F) Immunoprecipitation of nephrin from Robo2 knockout homozygous (*Robo2*^{-/-}), heterozygous (*Robo2*^{+/-}), and wild-type (*Robo2*^{+/+}) mouse kidneys using the anti-nephrin antibody. Note increased F-actin in lane 3.

(G) Intensity quantification of (F). Data are represented as mean \pm SEM; n =4, * p < 0.05 compared with the wild-type and heterozygous, ANOVA analysis. See also Figure S3.

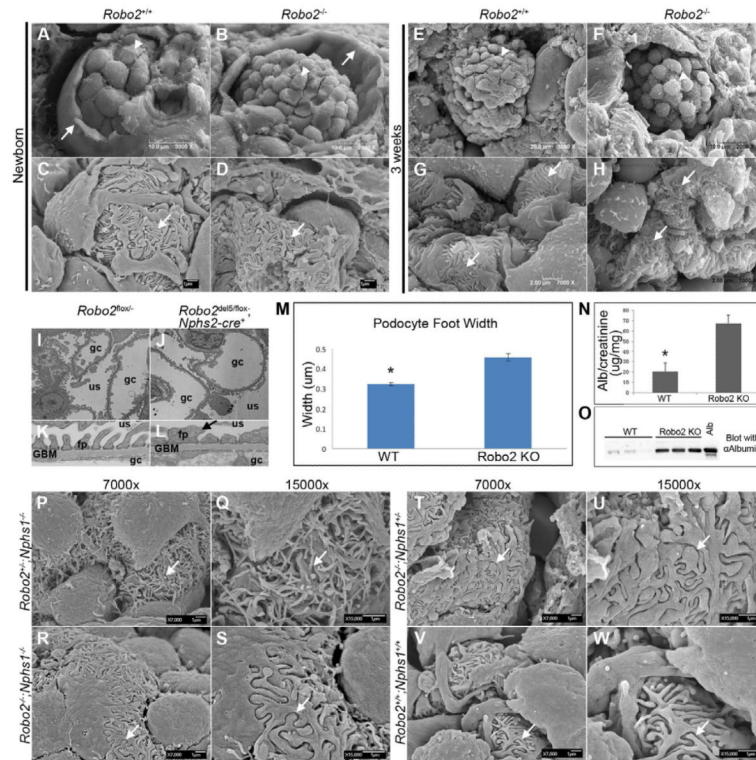


Figure 4. Podocyte structural phenotypes in the *Robo2* homozygous null, *Robo2* podocyte specific knockout, and *Robo2* and *Nphs1* double knockout mice

(A and B) Representative images of newborn kidneys show podocyte bodies (arrowheads) and Bowman's capsule (arrows) in wild-type (A) and *Robo2* homozygous null mice (B).

(C and D) High magnification images of (A and B) show podocyte foot processes (arrows) in the newborn kidney. Scale bar, 1 μ m

(E and F) Representative images of 3-week kidneys at low magnification show podocyte cell body (arrowheads) in a *Robo2* homozygous null mouse (F) compared to an age-matched control (E).

(G and H) Higher magnification images of (E and F) show disorganized shorter meandering foot processes (arrow) in a 3-week *Robo2* homozygous null mouse (H) compared to well-organized zip-like foot processes in the age-matched control (G). Scale bars: 2 μ m.

(I and J) Representative transmission electron microscopy images (magnification at 5000x) depict the focal segmental podocyte foot process effacement in a one month old *Robo2* podocyte-specific knockout mouse and the normal phenotype in the control (I).

Abbreviations: gc: glomerular capillary; us: urinary space.

(K and L) Higher magnification transmission electron microscopy images (40000x) show broader podocyte foot processes (arrow in L) in a two months old *Robo2* podocyte-specific mutant mouse compared with the control (K). Abbreviations: fp, podocyte foot process; GBM, glomerular basement membrane.

(M) Quantification of podocyte foot process width in one month old *Robo2*^{Δel5/flox}; *TgNphs2-Cre*⁺ podocyte specific knockout mice (Robo2 KO) and the wild-type littermate controls (WT). Data are represented as mean \pm SEM, $n=333$, * $p < 0.01$.

(N) ELISA assay of spot urine shows an elevated albumin/creatinine ratio in *Robo2*^{Δel5/flox}; *Nphs2-Cre*⁺ (KO) adult mice compared with control wild-type (WT). Data are represented as mean \pm SEM, $n=20$, * $p < 0.01$.

(O) Western blot analysis shows the presence of albumin in urine; 1 μ l urine was loaded on each well, 0.2 μ g albumin was used as a positive control. WT, three wild-type littermates; Robo2 KO, three individual *Robo2*^{del5/flox}; *Nphs2-Cre*⁺ mice.

(P and Q) Representative scanning electron microscope images show disrupted interdigitating podocyte foot processes that resemble disorganized cellular protrusions (arrows) in the *Nphs1*^{-/-} single homozygous newborn mouse kidney. Scale bars: 1 μ m.

(R and S) Glomeruli from *Nphs1*^{-/-}*Robo2*^{-/-} double homozygous newborn mice exhibit restored interdigitating foot processes (arrows), indicating alleviation of nephrin null phenotype by knocking out *Robo2*.

(T and U), Glomeruli from *Robo2*^{-/-} single homozygous newborn mice display irregular and broader foot processes but extensive interdigitating pattern formation (arrows).

(V and W), Glomeruli from newborn wild type mice with normal regular interdigitating pattern of the foot process (arrows). See also Figure S4 and Table S1-S4.